Analytical Methods

Accepted Manuscript

This article can be cited before page numbers have been issued, to do this please use: X. Lin, S. Li, B. Zhang, H. Yang, K. Zhang and H. Huang, *Anal. Methods*, 2020, DOI: 10.1039/D0AY01326A.

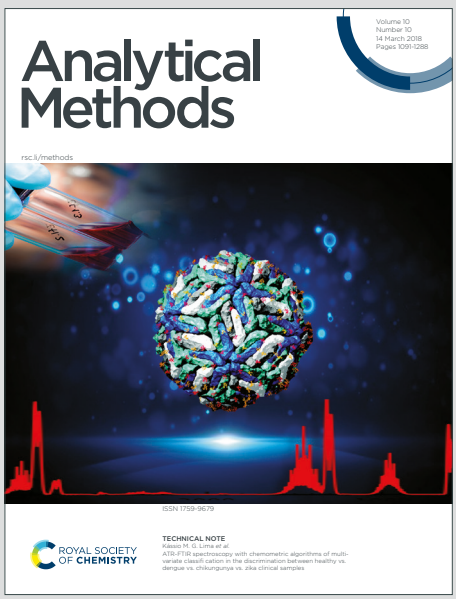

This is an Accepted Manuscript, which has been through the Royal Society of Chemistry peer review process and has been accepted for publication.

Accepted Manuscripts are published online shortly after acceptance, before technical editing, formatting and proof reading. Using this free service, authors can make their results available to the community, in citable form, before we publish the edited article. We will replace this Accepted Manuscript with the edited and formatted Advance Article as soon as it is available.

You can find more information about Accepted Manuscripts in the Information for Authors.

Please note that technical editing may introduce minor changes to the text and/or graphics, which may alter content. The journal's standard Terms & Conditions and the Ethical guidelines still apply. In no event shall the Royal Society of Chemistry be held responsible for any errors or omissions in this Accepted Manuscript or any consequences arising from the use of any information it contains.

View Article Online
DOI: 10.1039/D0AY01326A

Enzyme-free fluorescent biosensor for highly sensitive detection of carcinoembryonic antigen based on aptamer-induced entropy-driven circuit

Xiaojuan Lin,[a] Shengqiang Li,[b] Bogang Zhang,[c] Hua Yang,[a] Kai Zhang [a] and Hongge Huang *[a]

[a] Department of Clinical Laboratory, The Third Hospital of Xingtai, Xingtai, Hebei 054100, China

[b] Department of Clinical Laboratory, First Teaching Hospital of Tianjin University of Traditional Chinese Medicine, Tianjin 300000, China

[c] Department of Neurology, The Third Hospital of Xingtai, Xingtai, Hebei 054100, China

***Corresponding author.**

E-mail: xtsyhuanghongge@163.com

View Article Online
DOI: 10.1039/D0AY01326A

Abstract

Carcinoembryonic antigen (CEA) is a disease biomarker, which can reflect the existence of tumors. Accurate detection of CEA in clinical samples is highly valuable for diagnosis of tumors. Herein, we developed an enzyme-free fluorescent biosensor for highly sensitive detection of CEA based on aptamer-induced entropy-driven circuit. The aptamer hairpin specifically bound CEA to expose locked domain. Then, the exposed domain could trigger disassembly of multiple fluorophore strands from the three-strand complexes with the aid of fuel strands, leading to the production of remarkable amplified fluorescent signal. The one-step and homogeneous method exhibited high specificity and wide linear range from 10 pg mL^{-1} to 500 ng mL^{-1} with a low limit of detection of 4.2 pg mL^{-1}. What's more, the whole detection process could be performed with 45 min and did not involve the use of any protein enzymes and antibodies. The developed strategy could also be applied to detect CEA in clinical samples with satisfied results. Therefore, the strategy is an alternative sensing method for the detection of CEA.

Keywords: Aptamer; Entropy-driven circuit; Carcinoembryonic antigen; Fluorescence detection

View Article Online
DOI: 10.1039/D0AY01326A

Introduction

Tumor is a serious threat to human health, early diagnosis and early treatment is important to improve the prognosis of tumor patients. Carcinoembryonic antigen (CEA) is a glycoprotein of 180 kDa.[1] The level of CEA in serum of healthy people is generally lower than 5.0 ng mL^{-1}, while the level of CEA in tumor patients is higher.[2] Thus, CEA has been widely used as a biomarker for tumor screening. In addition, CEA also plays a central role in the staging, treatment monitoring, and prognosis evaluation of malignant tumors.[3] Therefore, highly sensitive detection of CEA is beneficial to early diagnosis and treatment of tumors.

Currently, a series of methods have been developed for the detection of CEA, including chemiluminescence immunoassay, electrochemiluminescence immunoassay, enzyme-linked immunosorbent assay, colorimetric immunoassay, electrochemical immunoassay, and fluorescence immunoassay.[4-10] In particular, fluorescent biosensors have attracted broad interest of scientists, and have been widely used to detect of proteins, cells, and nucleic acids due to the advantages of simple operation, high sensitivity, and fast response.[11] For example, Huang's group constructed a fluorescent immunoassay based on silver nanoparticles for the detection of CEA.[12] Zhang's group developed quantum-dot labeled antibodies for CEA detection.[13] Although these methods have high sensitivity, some defects still exist. For example, the preparation of nanoparticles suffers from tedious steps, so it is difficult to control the size and morphology. In addition, the use of protein antibodies increases the cost of testing and requires strict reaction conditions.

Aptamers are single-stranded DNA or RNA molecules screened from Systematic Evolution of Ligands by Exponential Enrichment (SELEX).[14] Aptamers bind to targeted molecules (metal ions, proteins, cells, and small molecules) with excellent affinity and specificity by forming secondary and tertiary structures.[15-19] Compared to antibodies, aptamers exhibit incomparable advantages, such as robust chemical stability, low immunogenicity, reversible denaturation and refolding.[20] Owing to the superior properties, these “chemical antibodies” have been extensively used as a universal platform to construct biosensing tools for the detection of various biomarkers.[21-26] Inspired by these attainments, we hypothesized that aptamer can be regarded as a potential substitution of CEA antibody.

With the rapid progress of DNA nanotechnology, many novel signal

View Article Online
DOI: 10.1039/D0AY01326A

amplification strategies have been developed, such as, hybridization chain reaction (HCR), catalytic hairpin assembly (CHA), and entropy-driven circuit (EDC).[27-29] In particular, EDC is an isothermal and enzyme-free reaction process, revealing prodigious potential for in vitro and in vivo applications.[30,31] Unlike CHA and HCR that depend on the interaction of multiple DNA hairpins, EDC achieves rapid signal amplification just by linear DNA molecules, avoiding background leakage brought by complex secondary structures of hairpins.[32,33] For example, Tan's group developed EDC-based nucleic acids biosensors, exhibiting low background noise, rapid amplification efficiency, and high stability.[34,35] Therefore, it is reasonable to speculate that EDC is very suitable for analyzing tumor biomarkers. However, its application in the detection of CEA is still lacking.

Aimed at this objective, we constructed a simple fluorescence sensing strategy based on aptamer-mediated EDC for highly sensitive detection of CEA in clinical samples. CEA bound and opened aptamers hairpins (AH) quickly and specifically, leading to the exposure of trigger strand for initiating EDC. As a result, numbers of fluorescent signals were generated by sequential strand displacement amplification. The combination of aptamers recognition and EDC endows the sensing strategy with high sensitivity and specificity. The enzyme- and antibodies-free biosensing method enabled detection of CEA in serum, and the results accorded closely with that from commercial Roche automatic electrochemiluminescence immunoassay analyzer. Therefore, we provided an alternative method for CEA detection.

Experimental

Materials and reagents

Carcinoma antigen 199 (CA199), carcinoma antigen 125 (CA125), CEA, and alpha-fetoprotein (AFP) were purchased from Linc-Bio Science Co. Ltd. (Shanghai, China). The serums of colon cancer patients and healthy persons were from the Third Hospital of Xingtai City. The reaction buffer of aptamer recognition and EDC (pH 7.4) contains 10 mM Tris(hydroxymethyl)aminomethane, 0.1 mM NaCl and 5.0 mM $MgCl_2$. All oligonucleotides were purchased from Sangon Inc. (Shanghai, China) and dissolved in TE buffer (pH 8.0, 10 mM Tris(hydroxymethyl)aminomethane hydrochloride (Tris-HCl), 1 mM ethylenediaminetetraacetic acid disodium salt (EDTA). These sequences were listed below. AH: 5'-*ATACCAGCTTATTCAATT*GCC CTTACTCCCTGAATAAGC-3'. Quencher

View Article Online
DOI: 10.1039/D0AY01326A

strand(Q):5'-GCTTATTCAGGGAGTAA GGGCAGGGCCGTAAGTTAGTTGGAGACGTAGG-quencher (BHQ1)-3'. Product strand (P): 5'-TTTTTTTTTTTTTTCCCTGCCCTTACTCCCTGA-3'. Reporter strand (R): 5'-fluorophore (FAM)-CCTACGTCTCCAACTAACTTACG-3'. Fuel strand (F): 5'-CCTACGTCTCCAACTAACTTACGGCCCTGCCCTTACTCCCTGA -3'. Italic DNA sequences represent CEA aptamer for capturing CEA. DNA sequences with underline in AH and Q can hybridize each other. The hybridization of Q, P, and R forms QPR complex. The hybridization of Q and F forms QF complex. 1 × TBE buffer (pH 8.3) contained 89 mM Tris - boric acid and 2 mM EDTA. All the water used in the experiment is Milli-Q water (≥ 18 MΩ Milli-Q).

Collection of serum from clinical samples

Blood samples included in this work were centrifuged (1500 × g, 5 min), and each 0.5 mL of the serum was transferred into a fresh 1.5 mL tube. These serums were stored at -80°C before use. All experiments were performed in accordance with the relevant laws and institutional guidelines of China (WS/T 225-2002), and approved by the ethics committee at The Third Hospital of Xingtai. Informed consents were obtained from human participants of this study.

Preparation of DNA probe

The three-stranded complex consisted of a FAM-labeled reporter strand (R), a BHQ1-labeled quencher strand (Q) and a product strand (P). The three strands with same concentration were mixed in 1 × TAE/Mg^{2+} buffer (1 mM EDTA, 40 mM Tris-Acetate, 12.5 mM $MgCl_2$, pH 8.0) at 95 ℃ for 5 minutes, then slowly decreased to room temperature. Similarly, the AH was heated to 95 ℃ for 5 minutes, then slowly decreased to room temperature. Finally, the three-stranded complex (QPR) and AH were stored at 4 ℃ before use.

Aptamer-induced EDC reaction

Different concentrations of CEA (25 μL) were added to the mixture of 25 μL of AH (250 nM), 25 μL of QPR (250 nM), and 25 μL of F (0.5 μM). Then, the mixtures were incubated at 37 ℃ for 45 min, followed by the measurement of fluorescence.

Fluorescence measurement

Quartz dish with an optical path length of 1.0 cm and Cary Eclipse Fluorescence Spectrophotometer (Agilent, California) were used for fluorescence detection. 480 nm was set as the excitation wavelength, and 490 - 600 nm as the fluorescence emission

spectrum. The width of the excitation and emission slit was set at 5 nm, and the maximum fluorescence emission intensity was 518 nm. Before each detection, the quartz dish was rinsed with 70% ethanol for 3 times, then with distilled water for 3 times, and dried with nitrogen.

Polyacrylamide gel electrophoresis (PAGE)

The volume of loading samples in each lane was 8 mL. The PAGE was conducted on electrophoresis analyzer (DYY-6C, Liuyi Instrument Company, China) with 8% native polyacrylamide gel in 1 × TBE buffer at 110 V for 45 min. After GoldView staining for 30 min, the gel was imaged on a Biorad ChemDoc XRS (Bio-Rad, U.S.A.).

Results and discussion

Principle of aptamer-induced EDC for CEA detection

Scheme 1 shows the principle of fluorescence biosensing method for CEA detection based on aptamer-induced EDC. The constituent of the sensing strategy only consists of QPR, F strand, and AH. The QPR complex includes three single-stranded DNA (Q, P, and R), in which Q and R are labeled by 3′-BHQ1 and 5′-FAM at the terminus, respectively. Q strand can hybridize with R strand and P strand, resulting in the fluorescence quenching of FAM through fluorescence resonance energy transfer (FRET). The AH contains green domain acted as CEA aptamer and pink domain served as trigger strand. CEA specifically binds to AH, leading to the formation of CEA@AH complex and the transformation of hairpin structure. Simultaneously, the pre-blocked trigger strand is exposed. Then, the exposed trigger strand binds to the 2* region of the QPR to form complex 1. With the strand displacement reaction, the P chain is replaced, forming complex 2 and exposing the 4* region in Q strand. Subsequently, the F strand hybridizes with the generated 4* region and then releases of R and trigger strand, forming complex 3. The released trigger strand propels the next EDC reaction. Therefore, large numbers of fluorescence signals are produced for CEA detection.

View Article Online
DOI: 10.1039/D0AY01326A

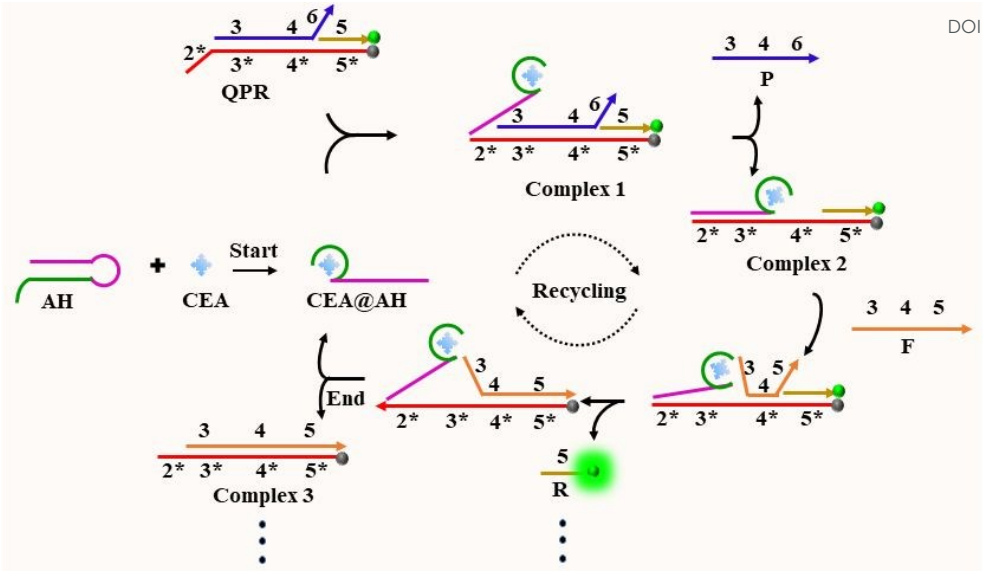

Scheme 1 Schematic illustration of fluorescence biosensing method based on aptamer-induced EDC for CEA detection.

Feasibility of the biosensing strategy

First, the binding of CEA and the AH was investigation. The AH was labeled by a quencher (3′-FAM) and fluorophore (5′-BHQ1) at its terminus. As shown in Fig. 1A, there was a weak fluorescence signal in the absence of CEA (curve a) due to 6-base distance between FAM and BHQ1, while an enhanced fluorescence signal was observed in the presence of CEA (curve b). These results suggested that CEA could bind to the AH, leading to the change of AH structure and the recovery of fluorescence of FAM. Second, the EDC reaction was verified by PAGE. As shown in Fig. 1B, lane 3 represented the synthesized trigger strand (T) that was used to mimic the strand exposed by the recognition of AH and CEA. The P strands, R strands, and Q strands were observed in lane 1, 2, and 5, respectively. Lane 4 represented the mixture of F strands and P strands, suggesting that the two substrates could stably exist. Owing to incomplete assembly, lane 6 showed multiple bands. Among them, the highest position was QPR complex. Upon the T was added into the mixture of F strands and QPR complex, the QPR complex obviously reduced and QF complex came out (lane 7). These results showed that the developed EDC reaction could successful operation and executed the task of signal amplification. Last, to verify the feasibility of this whole reaction for CEA detection, the fluorescence signal was

collected under different reaction conditions. As shown in Fig. 1C, the fluorescence intensity was ignorable in the presence of the QPR (curve a). When F chain was added to the mixture of AH and QPR, a slight increase in fluorescence signal was observed (curve b). This might be because the defective assembly of QPR could hybridize with F strand, leading to the release of a portion of R strand. However, a significantly enhanced fluorescence signal was observed in the presence of CEA (curve c). This was due to that CEA could specifically recognize the AH, leading to the initiation of the developed EDC reaction. These results clearly proved the feasibility of enzyme-free fluorescence method for CEA detection.

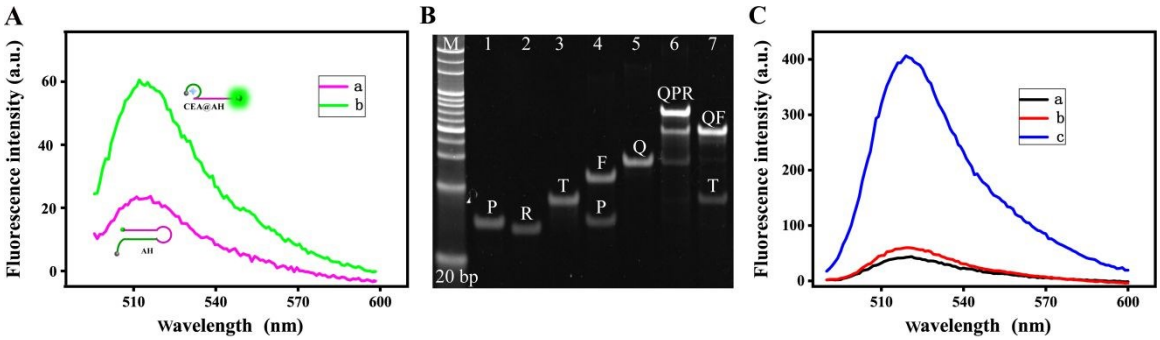

Fig. 1 Evaluation of the feasibility of the sensing strategy. (A)The interaction of CEA and the AH: (a) AH, (b) AH + CEA. (B) Verification of EDC by PAGE: (M) 20 bp marker, (1) P strands, (2) R strands, (3) T strands, (4) F strands + P strands, (5) Q strands, (6) QPR complex, and (7) T strands + QPR + F strands. The concentrations of all substrates were 2 μM. (C) Fluorescent biosensor response to different reaction conditions: (a) QPR, (b) AH + QPR + F, (c) CEA + AH + QPR + F. The concentrations of CEA, AH, QPR, and F were 500 ng mL^{-1}, 250 nM, 250 nM, and 500 nM, respectively. The reaction time was set at 50 minutes. The fluorophore for Figure 1B was the same as Scheme 1.

Optimization of the experiment conditions

To achieve the best performance of the designed biosensor, we systematically optimized four important experimental conditions. These conditions included the concentration of QPR complex, the ratio of QPR complex to F chain, reaction time, and reaction temperature. Because the concentration of QPR complex directly

affected the analytical performance of the sensing method (high concentration increased cost of detection, low concentration could not effectively trigger EDC reaction), we firstly optimized the concentration of QPR complex. As shown in Fig. 2A, when the concentration of QPR complex increased ranging from 10 nM to 250 nM, the fluorescence signal continually increased and reached to peak value at 250 nM, after which, the fluorescence signal remained unchanged. Fig. 2B illustrated the change in fluorescence signal with the ratio of QPR complex to F chain (QPR/F). When the ratio reached to 1:2, the fluorescence signal had the maximum value. To rapidly gain detection results, we further optimized the reaction time. As shown in Fig. 2C, the fluorescence signal underwent an upward trend from 15 minutes to 45 minutes and kept constant after 45 minutes. However, the background noise slowly increased with the increase of reaction time. It is well known that low temperature can reduce the reaction kinetics of EDC, while high temperature reduces the stability of QPR complex. Thus, the incubation temperature of this sensing strategy was also optimized. As depicted in Fig. 2D, with the increase of temperature, the signal increased gradually from 4 ℃ to 37 ℃. However, the background noise increased obviously after 37 ℃, leading to the distinct reduction of signal-to-noise ratio of the sensing method. According to the above experimental results, the concentration of QPR complex, the ratio of QPR complex to F chain, reaction temperature and reaction time were set to 250 nM, 1:2, 37 ℃, and 45 minutes, respectively. These optimized conditions were used to subsequent experiments.

View Article Online
DOI: 10.1039/D0AY01326A

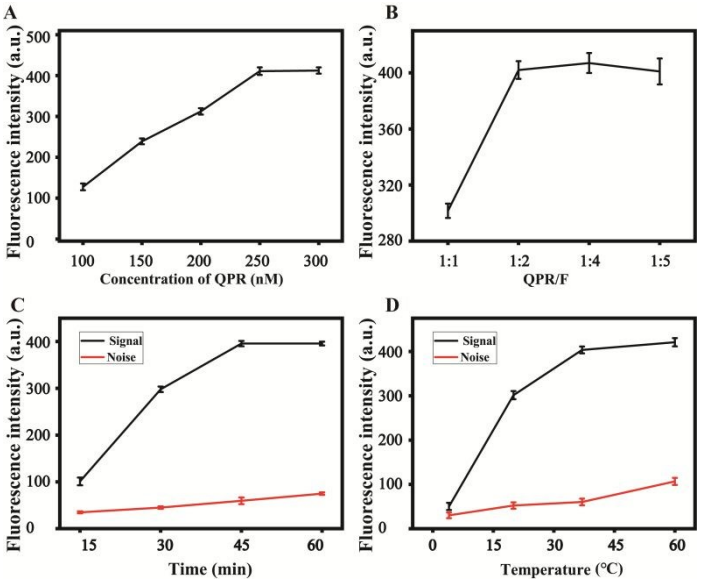

Fig. 2. Optimizations of experimental parameters. The effect of (A) QPR concentration, (B) the ratio of QPR concentration to F chain, (C) reaction time, and (D) reaction temperature on the fluorescence intensity of the biosensor. The concentrations of CEA and AH were 500 ng mL^{-1} and 250 nM, respectively. Data were expressed as mean ± standard deviations, sample replicates n = 3.

Sensitivity of the biosensor

Under the best experimental conditions, the analytical performance of the biosensor was evaluated by detecting different concentrations of CEA. As shown in Fig. 3A, the fluorescence intensity increased with the increase of CEA concentration from 0 to 500 ng mL^{-1}, indicating that the release of FAM-labeled R chain was highly related to CEA concentration. As shown in Fig. 3B, there was a good linear relationship between the logarithm of CEA concentration and fluorescence intensity ranging from 10 pg mL^{-1} to 500 ng mL^{-1}. The regression equation was F = 224.8 + 62.5lgC (R^2 = 0.9980), in which F represented fluorescence intensity and C represented CEA concentration. The limit of detection (LOD) of 4.2 pg mL^{-1} was evaluated based on a 3σb/slope, the σb stood for the standard deviation of three blank controls.[36] The LOD of this developed strategy was superior to that of magnetic induced surface-enhanced Raman scattering technique,[37] aptamer modified magnetic Fe_3O_4-Au nanoparticles,[38] and electrochemical immunosensor based on gold

nanoparticles and multi wall carbon nanotubes.[39] On the other hand, the LOD of the biosensor was comparable to that of fluorescent and electrochemical biosensors based on carbon nanotube and carboxyl functionalized CdSe nanocrystals.[40] Moreover, the sensitivity of this strategy was higher than that of commercial Roche automatic electrochemiluminescence immunoassay analyzer (200 pg mL^{-1}). The detailed comparison was shown in Table 1. The good analytical performance of the method was attributed to the recognition specificity of aptamer and the efficient signal amplification ability of EDC reaction.

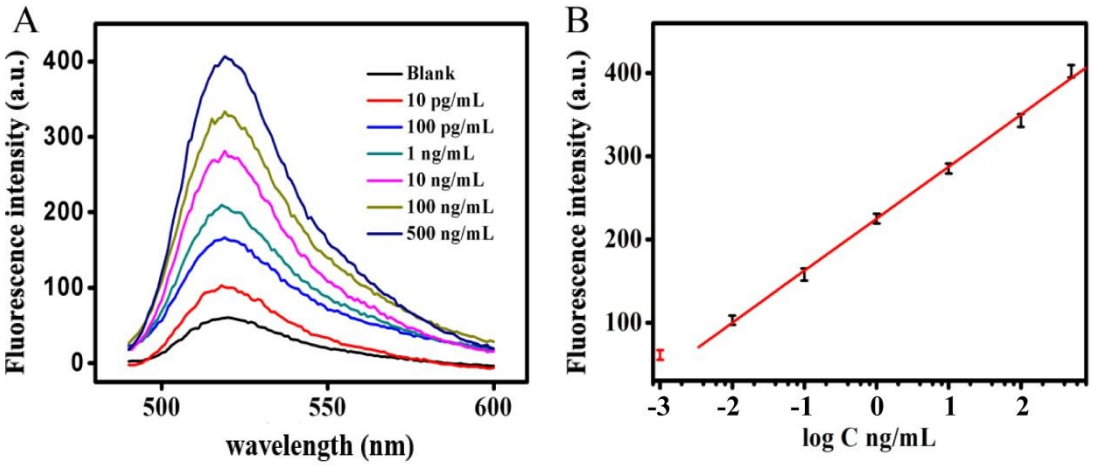

Fig. 3. Evaluation of the sensitivity of the strategy. (A) Fluorescence spectra corresponding to different concentrations of CEA. (B) Linear relationship between logarithm of CEA concentration and fluorescence intensity. Data were expressed as mean ± standard deviations, sample replicates n = 3.

Table 1. Comparison with recent methods for CEA detection.

Methods	Strategies	Detection range	LOD	Refs.
SERS	MBs and AuNPs	50-2000 mL^{-1}	20 pg mL^{-1}	37
Nanopore	Magnetic Fe_3O_4-AuNPs	2-200 ng mL^{-1}	0.6 ng mL^{-1}	38
Electrochemistry	AuNPs and MWCNTs	0.4-125 ng mL^{-1}	0.09 ng mL^{-1}	39
Fluorescence/ Electrochemistry	Carbon nanotube and CdSe nanocrystals	1-20 pg mL^{-1}/ 5-50 pg mL^{-1}	0.25 pg mL^{-1}/ 1.7 pg mL^{-1}	40
Electrochemistry	Pt@CuMOFs-hGq-GOx	0.05 pg mL^{-1} - 20	0.023 pg mL^{-1}	41

View Article Online
DOI: 10.1039/D0AY01326A

		ng mL^{-1}		
Electrochemistry	PtPdNWs, MnTMPyP, and HCR	0.1 pg mL^{-1} - 40 ng mL^{-1}	0.030 pg mL^{-1}	42
Fluorescence	Aptamer-induced EDC	10 pg mL^{-1} - 500 ng mL^{-1}	4.2 pg mL^{-1}	This work

SERS: surface-enhanced Raman scattering; MBs: magnetic beads; MWCNTs: multi wall carbon nanotubes; AuNPs: Au nanoparticles. Pt@CuMOFs-hGq-GOx: Cu-based metal-organic frameworks functionalized with Pt nanoparticles, aptamer, hemin and GOx; PtPdNWs: PtPd nanowires; MnTMPyP: manganese (III) meso-tetrakis (4-N-methylpyridiniumyl)-porphyrin; HCR: hybridization chain reaction.

Specificity, repeatability, and stability of this strategy

To evaluate the specificity of the fluorescence sensor, some tumor markers (CA125, CA199, and AFP) were used as interferents. As shown in Fig. 4A, only weak fluorescence signals were observed in the presence of CA125, CA199, and AFP, respectively. However, a significantly enhanced fluorescence signal was observed in the presence of CEA. When CEA was added into the mixture of CA125, CA199, and AFP, the fluorescence signal did not change obviously. These results showed that this method had good selectivity and was not affected by other high concentration of tumor biomarkers. To evaluate the repeatability of this biosensor, we measured five samples containing 1.0 ng mL^{-1} CEA (Fig. 4B). The relative standard deviation (RSD) value was evaluated as 2.5%, suggesting that the biosensor had good reproducibility. In addition, the stability of this biosensor was assessed. As shown in Fig. 4C, the fluorescence signals did not reduce in five days (d). Even if the components of the biosensor were left for ten days at 4 ℃, the fluorescence intensity only dropped by 12.5%. Thus, the developed biosensor had acceptable stability.

View Article Online
DOI: 10.1039/D0AY01326A

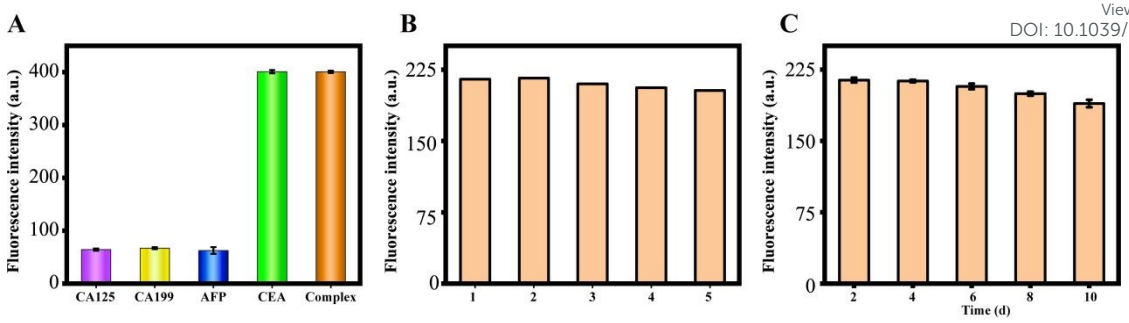

Fig. 4. Investigation of (A) the specificity, (B) repeatability, and (C) stability of the biosensor. In the test of specificity, the concentrations of CA125, CA199, and AFP were 5.0 μg mL^{-1}, respectively, and the concentration of CEA was 0.5 μg mL^{-1}. In the test of stability, the concentration of CEA was 1.0 ng mL^{-1}. Data were expressed as mean ± standard deviations, sample replicates n = 3.

Real Sample Analysis

In order to evaluate the availability of this method, various known concentrations of CEA were spiked into healthy human serum to conduct the recovery test. The closer the assayed value of this method is to the added CEA value, the higher the accuracy of this method. Table 2 showed that the recovery rates were between 99.0% and 110.0%, and the RSD ranged from 2.51% to 3.12%. To further demonstrate the practicability, the serums of colon cancer patients were tested by the developed biosensor and commercial Roche automatic electrochemiluminescence immunoassay analyzer. As shown in Fig. 5, the results from the developed biosensor (a, c, and e) were consistent with that from commercial analyzer (b, d, and f). These results proved that the biosensor could be used for the detection of CEA in clinical samples.

Table 2. Recovery test using the developed biosensor.

Samples	Added CEA value (ng mL^{-1})	Assayed CEA value (ng mL^{-1})	Recovery (%)	RSD (%)
1	0.100	0.100	100	3.12
2	1.00	1.10	110	2.51
3	10.0	9.90	99.0	2.93

4	100	99.8	99.8	2.62

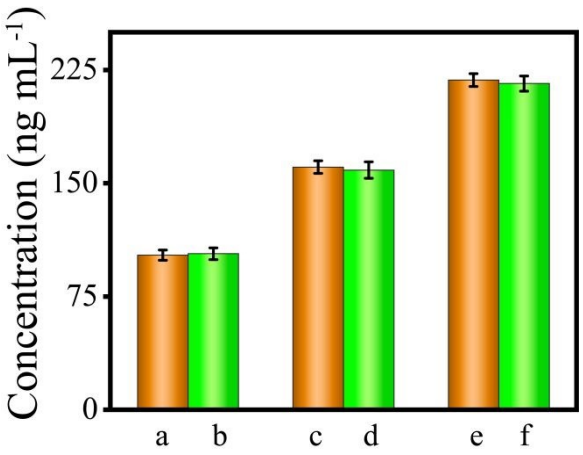

Fig. 5. Demonstration of the practicability of the biosensor. The results of a, c, and e were gained by the biosensor we developed. The results of b, d, and f were gained by commercial analyzer. The serums were from three colon cancer patients. Data were expressed as mean ± standard deviations, sample replicates n = 3.

Conclusions

In summary, an enzyme-free, highly sensitive sensing strategy based on aptamer-induced EDC has been successfully developed for the detection of CEA. Owing to the combination of aptamer recognition and EDR reaction, this method has high specificity and sensitivity. Compared with the previous sensing methods for CEA detection, the method we developed does not require complicated sequence design, tedious synthesis of nanomaterials, and multiple detection steps, which can ensure the repeatability of detection. Furthermore, the biosensor has not the participation of antibodies and protein enzymes, thus saving the cost of detection. In addition, the sensing strategy can accurately detect the concentration of CEA in clinical samples. Therefore, this method has the advantages of simple, enzyme-free and one-step detection, and possesses the potential to serve as an alternative tool for the detection of CEA.

Conflicts of interest

There are no conflicts to declare.

Acknowledgements

View Article Online
DOI: 10.1039/D0AY01326A

This research was supported by the "new development project" of the First Teaching Hospital of Tianjin University of Traditional Chinese Medicine (201905).

References

1 P. Thomas, A. Gangopadhyay, G. Steele Jr, C. Andrews, H. Nakazato, S. Oikawa and J. M. Jessup, *Cancer Lett*., 1995, **92**, 59.

2 X. Gu, Z. She, T. Ma, S. Tian and H. B. Kraatz, *Biosens. Bioelectron*., 2018, **102**, 610.

3 F. Naghibalhossaini and P. Ebadi, *Cancer Lett*., 2006, **234**, 158.

4 J. H. T. Luong and S. K. Vashist, *Biosens. Bioelectron*., 2017, **89**, 293.

5 Y. Yu, Q. Zhang, J. Buscaglia, C. C. Chang, Y. Liu, Z. Yang, Y. Guo, Y. Wang, K. Levon and M. Rafailovich, *Analyst*, 2016, **141,** 4424.

6 D. Wang, Y. Li, Z. Lin, B. Qiu and L. Guo, *Anal. Chem*., 2015, **87**, 5966.

7 A. Jing, Q. Xu, W. Feng and G. Liang, *Micromachines*, 2020, **11**, E660.

8 W. Li, C. Ma, Y. Song, C. Hong, X. Qiao and B. Yin, *Nanotechnology*, 2020, **31**, 185605.

9 Y. Song, W. Li, C. Ma, Y. Sun, J. Qiao, H. Li and C. Hong, *Sens. Actuators B Chem.*, 2020, **319**, 128311.

10 J. Liu, J. Wang, Z. Li, H. Meng, L. Zhang, H. Wang, J. Li and L. Qu, *Microchim. Acta*, 2018, **185**, 110.

11 X. Huang, Y. Liu, B. Yung, Y. Xiong and X. Chen. *ACS Nano*, 2017, **11**, 5238.

12 N. U. Khan, Z. Feng, H. He, Q. Wang, X. Liu, S. Li, X. Shi, X. Wang, B. Ge and F. Huang. *Anal. Chim. Acta*, 2018, **1040**, 120.

13 Y. Chen, X. Guo, W. Liu and L. Zhang, *Mikrochim. Acta*, 2019, **186**, 112.

14 R. Stoltenburg, C. Reinemann and B. Strehlitz. *Biomol. Eng.*, 2007, **24**, 381

15 A. B. Iliuk, L. Hu and W. A. Tao, *Anal. Chem*., 2011, **83**, 4440.

16 F. Wang, J. Dai, H. Shi, X. Luo, L. Xiao, C. Zhou, Y. Guo and D. Xiao, *Anal. Methods*, 2020, **12**, 2215.

17 M. Jarczewska and E. Malinowska, *Anal. Methods*, 2020, **12**, 3183.

18 P. Ding, Z. Wang, Z. Wu, W. Zhu, L. Liu, N. Sun and R. Pei, *J. Mater. Chem. B*.,

View Article Online
DOI: 10.1039/D0AY01326A

2020, **8**, 3408.

19 Y. Li, L. Sun and Q. Zhao, *Anal. Chem.*, 2019, **91**, 2615.

20 H. Ma, J. Liu, M. M. Ali, M. A. Mahmood, L. Labanieh, M. Lu, S. M. Iqbal, Q. Zhang, W. Zhao and Y. Wan, *Chem. Soc. Rev*., 2015, **44**,1240.

21 Y. Jiang, M. Shi, Y. Liu, S. Wan, C. Cui, L. Zhang and W. Tan, *Angew. Chem. Int. Ed. Engl*., 2017, **56**, 11916.

22 D. Ye, M. Li, T. Zhai, P. Song, L. Song, H. Wang, X. Mao, F. Wang, X. Zhang, Z. Ge, J. Shi, L. Wang, C. Fan, Q. Li and X. Zuo, *Nat. Protoc*., 2020, 15, 2163

23 W. Xiang, Q. Lv, H. Shi, B. Xie and L. Gao, *Talanta*, 2020, **214**, 120716.

24 R. Zhang, L. Liu, D. Mao, D. Luo, F. Cao, Q. Chen and J. Chen, *Bioelectrochemistry*, 2020, **133**, 107492.

25 J. Wang, X. Guo, R. Liu, J. Guo, Y. Zhang, W. Zhang and S. Sang, *Nanotechnology*, 2019, **31**, 015501.

26 Z. Hong, G. Chen, S. Yu, R. Huang and C. Fan, *Anal. Methods*, 2018, **10**, 5364.

27 W. Chen, X. Zhang, J. Li, L. Chen, N. Wang, S. Yu, G. Li, L. Xiong and H. Ju, *Anal. Chem*., 2020, **92**, 2714.

28 Z. Qing, J. Xu, J. Zheng, J. Zheng, L. He, Z. Zou, S. Yang, W. Tan and R. Yang, *Angew. Chem. Int. Ed. Engl*., 2019, **58**, 11574.

29 H. Shi, J. Dai, F. Wang, Y. Xia, D. Xiao and C. Zhou, *Anal. Methods*, 2020, **12**, 2779.

30 D. Li, X. Li, B. Shen, P. Li, Y. Chen, S. Ding and W. Chen, *Anal. Chim. Acta*, 2019, **1092**, 102.

31 Y. Kitamura, Y. Azuma, Y. Katsuda and T. Ihara, *Chem. Commun*., 2020, **56**, 3863

32 C. Zhang, Z. Wang, Y. Liu, J. Yang, X. Zhang, Y. Li, L. Pan, Y. Ke and H. Yan, *J. Am. Chem. Soc.*, 2019, **141**, 17189

33 J. Yang, R. Wu, Y. Li, Z. Wang, L. Pan, Q. Zhang, Z. Lu and C. Zhang, *Nucleic Acids Res.*, 2018, **46**, 8532.

34 Y. Lv, L. Cui, R. Peng, Z. Zhao, L. Qiu, H. Chen, C. Jin, X. B. Zhang and W. Tan,

View Article Online
DOI: 10.1039/D0AY01326A

Anal. Chem., 2015, **87**, 11714.

35 L. He, D. Lu, H. Liang, S. Xie, X. Zhang, Q. Liu, Q. Yuan and W. Tan, *J. Am. Chem. Soc.*, 2018, 140, 258.

36 Y. Xiong, J. Zhang, Z. Yang, Q. Mou, Y. Ma, Y. Xiong and Y. Lu, *J. Am. Chem. Soc.*, 2020, **142**, 207.

37 X. R. Bai, L. H. Wang, J. Q. Ren, X. W. Bai, L. W. Zeng, A. G. Shen and J. M. Hu, *Anal. Chem.*, 2019, **91**, 2955.

38 H. Tang, H. Wang, C. Yang, D. Zhao, Y. Qian and Y. Li, *Anal. Chem.*, 2020, **92**, 3042.

39 G. Paimard, M. Shahlaei, P. Moradipour, H. Akbari, M. Jafari and E. Arkan, *Sens. Actuators B Chem.*, 2020, **311**, 127928.

40 Y. Zhao, X. Cai, C. Zhu, H. Yang and D. Du, *Anal. Chim. Acta*, 2020, **1096**, 61.

41 X. Zhou, S. Guo, J. Gao, J. Zhao, S. Xue and W. Xu, *Biosens. Bioelectron.*, 2017 **98**, 83.

42 X. Zhou, S. Xue, P. Jing and W. Xu, *Biosens. Bioelectron.*, 2016, **86**, 656.